Reference PMHS Tests to Assess Whole-Body Pedestrian Impact Using a Simplified Generic Vehicle Front-End

Eric Song, Jerome Uriot, Pascal Potier, Denis Dubois, Philippe Petit, Xavier Trosseille, Richard Douard

Abstract This study aims to provide reference post-mortem human subject tests, with easily reproducible test conditions, for whole-body pedestrian impact. A generic buck was developed to represent a mid-size sedan front-end. It was composed of three cylindrical steel tubes, representing the bonnet leading edge, bumper and spoiler, respectively. Four post-mortem human subjects were impacted laterally in a mid-gait stance by the buck at 8 m/s. Kinematics of the subjects were recorded via high-speed videos. Impact forces between the subjects and the buck were measured via load cells behind each tube; femur and tibia deformation and fractures were monitored via gauges on these bones. Biofidelity corridors were then established in terms of pedestrian kinematics and impact force between the subjects and the buck. Simplicity of its geometry and use of standard steel tubes for the buck will make it easy to perform future, new post-mortem human subject tests in the same conditions, or to assess dummies or computational models using these reference tests.

Keywords Pedestrian, Impact, cadaver, Dummy, Model.

I. INTRODUCTION

Development of dummies and computational models requires biofidelity targets for their validation. Tests on post-mortem human subjects (PMHS) remain the primary source of establishing such targets for pedestrian impacts. The impact severity, generally required to be at injury levels, bans any tests with human volunteers. A series of biofidelity targets was developed in the past, based on body region impactor tests, such as in [1-2]. However, this type of testing does not address interactions between body regions and their effects on the overall pedestrian kinematics, dynamics and injury risk. For example, the head impact against the vehicle is conditioned by that of limbs with the spoiler, the bumper and the bonnet leading edge (BLE). So it is necessary to perform full-scale pedestrian-vehicle tests in order to cover this gap.

A series of full-scale pedestrian-vehicle tests was performed by Kerrigan *et al*. [3-5]. In these tests, production vehicles were cut just rearward of the B-pillar, vehicle wheels were removed and the front suspension was locked. The vehicle bucks were then mounted to a sled and propelled to impact PMHS in a mid-gait stance. These tests provided valuable data relative to pedestrian kinematics and injury risk. However, in order to use these data to assess biofidelity of dummies and computational models, it is necessary to find the same production vehicle for physical testing, and to get the corresponding numerical vehicle model for computational simulations. This necessity limits, to some extent, the use of these data by a larger community.

Considering the above limitations, the use of a simplified generic vehicle represents a good alternative to perform full-scale pedestrian-vehicle tests and to generate biofidelity targets that are easier to be used and duplicated for physical tests and computational simulations. Following such consideration, a generic buck representing the front end of a small sedan was developed by Pipkorn *et al*. [6-7] and by Takahashi *et al.* [8]. It is composed of deformable components, including the lower bumper, upper bumper, grill, BLE, bonnet and windshield. Three PMHS tests using this buck were performed by Forman *et al*. [9-10]. In these tests, the subjects were positioned in a mid-gait stance and impacted on their right by the buck at a velocity of 40 km/h. Based on these three tests, biofidelity corridors on pedestrian kinematics and on impact forces between pedestrian and buck were established for a 50th percentile male pedestrian.

The aim of this study was to develop biofidelity corridors by performing PMHS tests with a much more simplified vehicle buck, which could be easily reproduced and numerically simulated. The buck was composed of

E. Song (e-mail: eric.song@lab-france.com; tel: + 33-1-76-87-36-42), P. Petit and X. Trosseille are Senior Researchers in Biomechanics at LAB PSA Renault in Nanterre, France. J. Uriot is a Senior Researcher, and P. Potier and D. Dubois are experimentation specialists in Biomechanics at CEESAR, France.. R. Douard is a Professor of Medicine at Université René Descartes, Paris.

three cylindrical steel tubes, representing the spoiler, bumper and BLE, respectively. Four PMHS were impacted on their right and in a mid-gait stance by the buck at 8 m/s. Kinematics of the subjects were recorded via high-speed videos. Impact forces between the subjects and the buck were measured via load cells behind each tube; femur and tibia deformation and fractures were monitored via gauges on these bones. Biofidelity corridors were then established in terms of pedestrian kinematics and impact force between the subjects and the buck.

II. METHODS

In this paper, the laboratory coordinate system is defined as follows: the positive X-axis is directed to the buck; the positive Z-axis is directed upward; and the GHBMC 50th percentile simplified pedestrian model (GHBMC_M50_PS) was used as a representation of the 50th percentile male pedestrian (M50), in order to position PMHS, to scale kinematic responses and to illustrate the test set-up and instrumentations used.

Vehicle buck

A generic vehicle buck was first developed at LAB (Fig. 1). It consisted of three steel cylindrical tubes screwed on rigid supports in V-form, representing the spoiler, bumper and BLE of a vehicle, respectively (named as LAB 3C buck in the following text). The tubes were positioned to represent a mid-size European sedan front-end. All three tubes had identical dimensions: 450 mm in length, 110 mm in outer diameter and 1.2 mm in thickness. These dimensions were determined in order that: (1) the tubes were long enough to recruit all two legs during an impact; and (2) the buck frontal stiffness remained representative of a sedan.

All these components were mounted on a pneumatic mini-sled. The mini-sled, with a total mobile mass of 150 kg, was propelled to 8 m/s to impact four PMHS on their right. After a free race of 650 mm, the mini-sled was progressively stopped via four belts with load limiter of 4kN. Each belt was attached to the mini-sled in one end and was fixed with respect to the ground in the other end, with a belt slack of 650 mm on the other end (Fig.2). Fig. **2** shows displacement and velocity time histories of the mini-sled corresponding to the four PMHS tests.

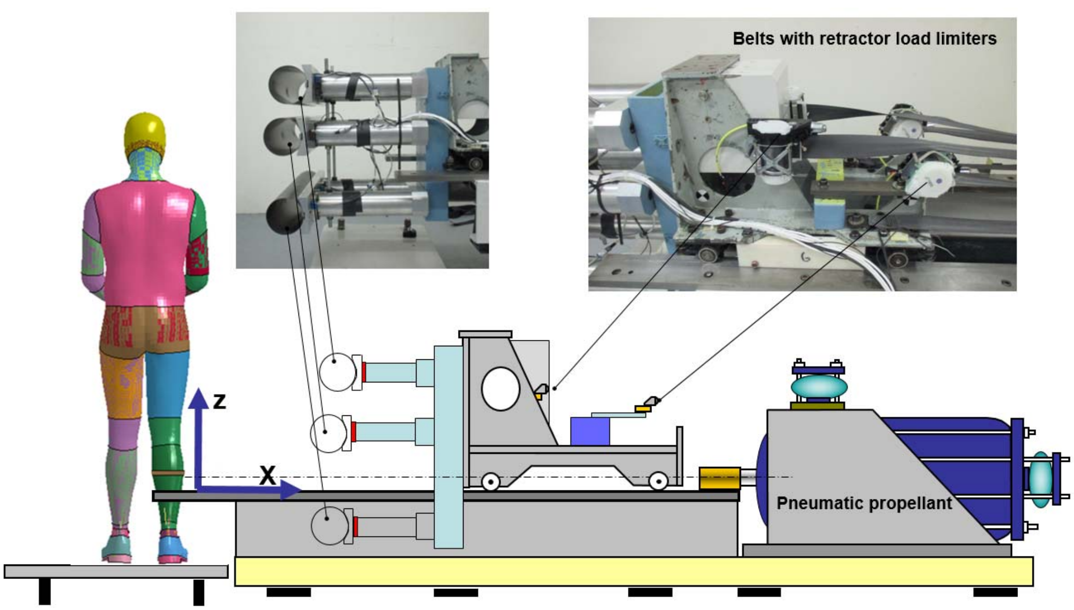

Fig. 1. General illustration of the simplified generic vehicle front-end (LAB 3C buck) and the PMHS position represented by the GHBMC 50th percentile simplified pedestrian model. PMHS positioning section provides more information regarding the simulated ground.

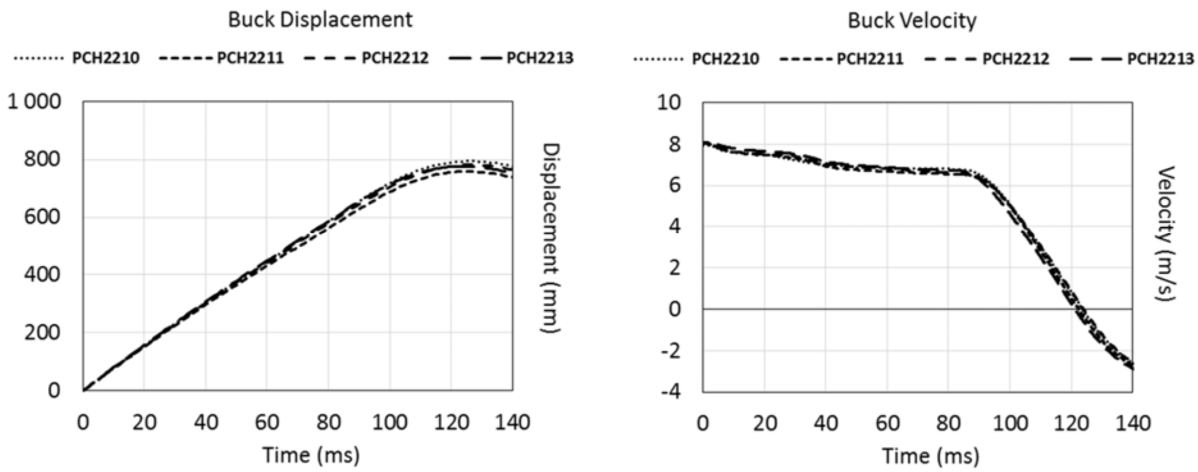

Fig. 2. Displacement and velocity time histories of the LAB 3C buck corresponding to the four PMHS tests.

The reaction force behind each contact area was measured by means of two load cells positioned under a V-form part supporting the tube (Fig. 3). The acceleration of each V-form along the x-axis was also measured. For each area, inertial force was first calculated using the acceleration and the mass in frontal of the load cell, then it was added to the reaction force to get the impact force sustained by the pedestrian.

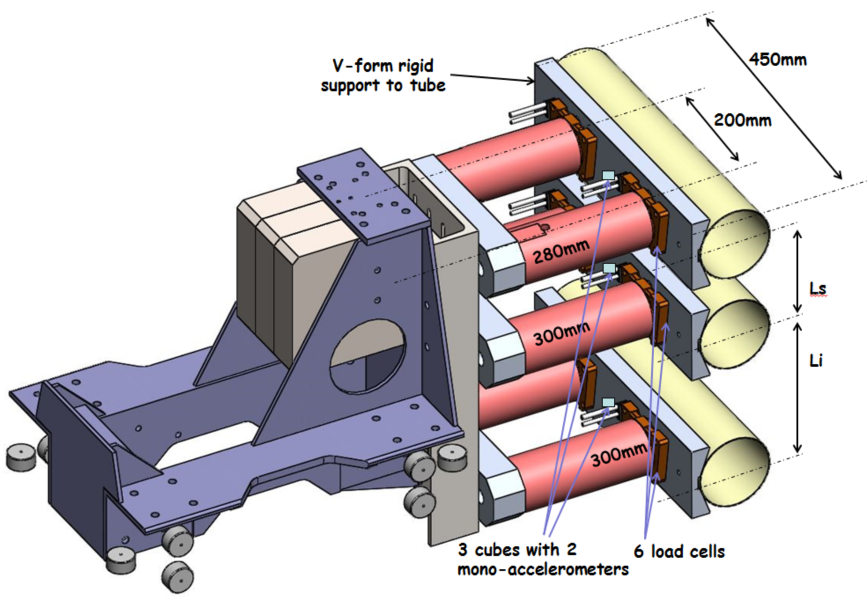

Fig. 3. Impact force measurement set-up.

PMHS preparation

Four PMHS tests were performed with the buck described above. Table I shows characteristics of these tests. They were obtained through the Body Donation to Science system at the Saints Pères University of Medicine, Paris, and the experimental protocol was approved by the Ethics Committee of the University. During the PMHS selection process, all PMHS were tested and found negative for Cytomegalovirus, B and C Hepatitis Virus, and Human Immunodeficiency Virus. Furthermore, they were CT-scanned and checked for metastases or other bony lesions prior to testing. PMHS were stored in a freezer (-15 degrees C) until they were removed and defrosted at room temperature for 48-72 hours prior to the pre-test preparation. During the tests, PMHS were clothed with an integral red suit and with lightweight general-purpose shoes.

TABLE I
TEST MATRIX AND CHARACTERISTICS OF PMHS USED

Test #	Subject #	Configuration	Sex	Mass (kg)	Height (cm)	BMI (kg/m2)	Age
PCH2210	MS686	LAB 3C buck	M	60	178	18.9	83
PCH2211	MS687	LAB 3C buck	M	79	171	27.0	77
PCH2212	MS688	LAB 3C buck	M	88	178	27.8	71
PCH2213	MS689	LAB 3C buck	M	81	173	27.1	87

Each PMHS was instrumented with six mono-axis strain gauges on its right femur and tibia (impacted in the first place) in order to: (1) record the precise moments of bone fractures should they occur; and (2) to estimate the moments in corresponding bone sections. As shown in Fig. 4, three gauges were installed on the media surface of the femur along its longitudinal direction and at the junction epiphysis/diaphysis, at the middle of the diaphysis, and at the junction diaphysis/inferior epiphysis, respectively. In the same way, three gauges were also installed on the right tibia.

Two types of photo target were used to track PMHS kinematics: (1) 2D targets stuck on the cloth surface; and (2) 3D targets (spheres) screwed on PMHS bones. However, 2D targets on the knee were sewed to the skin since the cloth may slide significantly at these locations. Fig. **5** shows all photo targets used. Corridors for the targets indicated in Table II were constructed and presented in the results section.

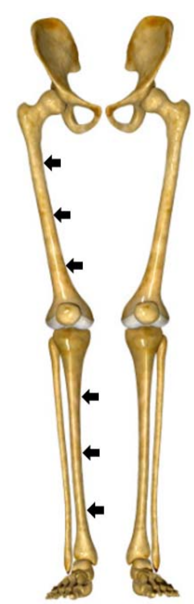

Fig. 4. Locations where strain gauges were installed.

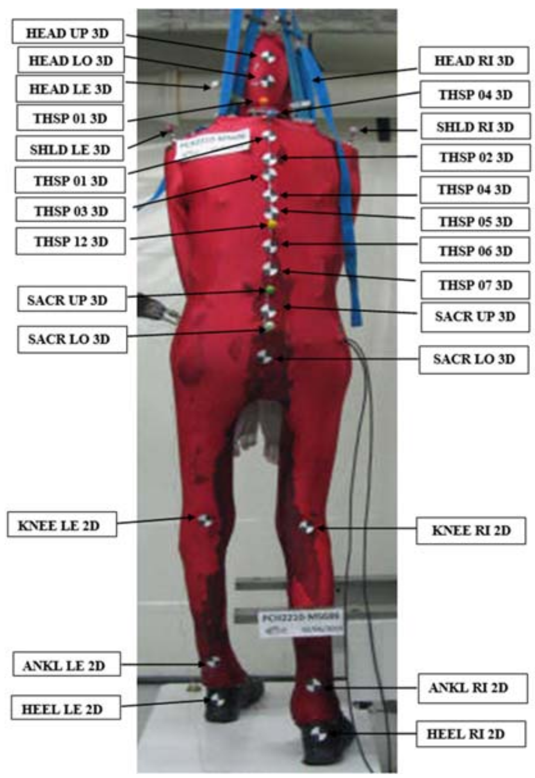

Fig. 5. Photo targets for kinematic tracking.

TABLE II
PHOTO TARGETS USED TO CONSTRUCT KINEMATICS CORRIDORS

Photo target	Type
Head centre left	3D
Acromion left	3D
T1	3D
T4	3D
T12	3D
Super sacrum	3D
Lower sacrum	3D
Knee	2D
Ankle	2D

Four cameras were used to track motion of those targets: a posterior view covering body regions from the head to the knees; a second posterior view covering the pelvis and the limbs; a right-angled posterior view of the whole body; and a left-angled posterior view of the whole body. The cameras captured 2000 frames per second with a 1024 x 1024 resolution.

PMHS positioning

The PMHS were initially positioned in a mid-gait stance, with the right leg back and the left leg forward. They were oriented relative to the buck such that they were struck laterally on the subject’s right side. In order to determine the z position of each PMHS versus the buck, a target position, shown in Fig. 6, was first defined for a

50th percentile male pedestrian (M50). This position was determined in such a way that the bumper tube centre was at the same height as the right knee target, which is located 10 mm distal from the tibia plateau and centered relative to the anterior and posterior edges of the tibia plateau. This right knee target will be referred to as the anatomical reference in the following texts.

For a PMHS of a size other than M50, its positioning followed the principles set out below:

- Relative position in Z (defined by Ls, Li) between the BLE, bumper and spoiler was scaled in function of the lengths of the thigh and the lower leg (Equations 1–4).

$$\lambda_{s\_j} = \frac{L_{M50\_thigh}}{L_{j\_thigh}} \quad (1)$$

$$\lambda_{i\_j} = \frac{L_{M50\_leg}}{L_{j\_leg}} \quad (2)$$

$$L_{s\_j} = \frac{L_s}{\lambda_{s\_j}} \quad (3)$$

$$L_{i\_j} = \frac{L_i}{\lambda_{i\_j}} \quad (4)$$

where L_{M50_thigh} (475 mm) and L_{M50_leg} (472 mm) are reference M50 thigh and lower leg lengths; L_{j_thigh} and L_{j_leg} are corresponding lengths for the j_{th} subject; L_s (150 mm) and L_i (230 mm) are reference height differences between the BLE and the bumper, and between the bumper and the spoiler for M50; L_{s_j} and L_{i_j} are corresponding height differences for the j_{th} subject; λ_{s_j} and λ_{i_j} are corresponding length scaling coefficients.

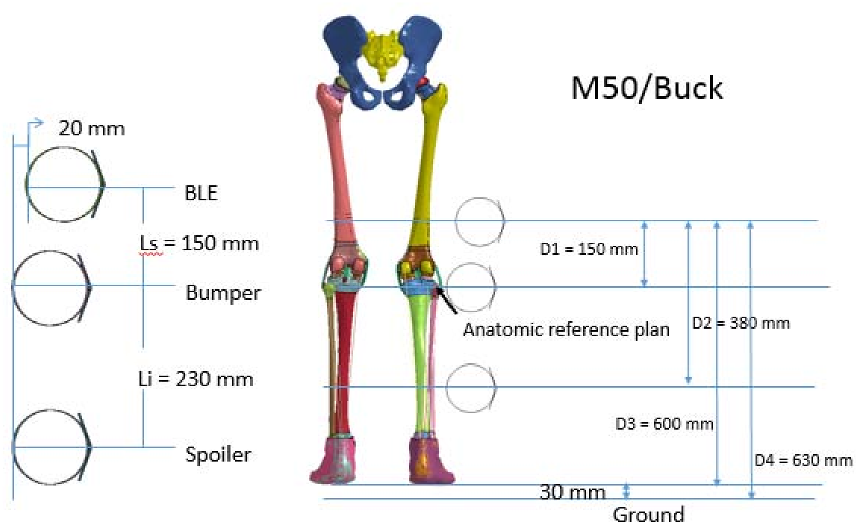

Fig. 6. Relative position between the buck and the M50; buck profile was scaled vs each PMHS thigh and lower leg lengths.

The reference M50 thigh length is that from the femur head extremity to the tibia plateau, and the reference M50 lower leg length is that from the tibia plateau to the foot bottom face. Note that:

- There was no scaling regarding the relative position in X between the BLE, bumper and spoiler tubes and their diameters.

- The BLE position was fixed; the position in Z of the spoiler, bumper and foot support were adjusted according to above scaling for each specific PMHS test.
- Each PMHS was positioned by aligning its anatomic reference to the bumper centre.

The subjects were maintained in their vertical position from above via a harness system. The harness belt was fixed to a device, which allows for: (1) adjusting its positions along the y-axis; (2) measuring the traction force to maintain the subject; (3) quick-release of the subjects via electrical magnets. The subjects were supported from underneath via a marble slab. The slab was superposed by a plate of Teflon in order to minimize friction effects between the feet and the support. The height of the marble was adjustable via four screws, allowing adjustment of the vertical position of the subjects. The feet were stabilized by pulling strings on their shoes. Note that the fixation of the strings was fragile in order not to affect the lower leg response.

Legs were positioned based on the following criteria, in order of diminishing importance.

- Criterion 1: the right and left knees do not overlap from lateral view.
- Criterion 2: the z position of the anatomic reference is aligned with the centre of the bumper.
- Criterion 3: the angles of the tibia and femur are as close as possible to the targets defined in Fig. 7. These angles correspond to those of leg bones of the GHBMC 50th percentile male pedestrian model positioned according to the positioning guidelines in SAE J2782.
- Criterion 4: the feet are stable on its support surface before the impact.
- Criterion 5: the legs are as perpendicular to the ground as possible in the plane OXZ.

TABLE III indicates the final leg positions obtained following the above procedure.

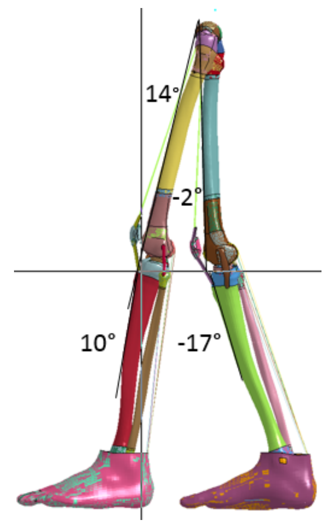

Fig. 7. Target angles for PMHS leg positioning and based on GHBMC_M50_PS.

TABLE III
FINAL LEG POSITION/ORIENTATION OBTAINED FOLLOWING THE ABOVE TEST PROCEDURE

Test #	Subject #	Anatomic ref./ Bumper*	Right femur	Right tibia	Left femur	Left tibia
PCH2210	MS686	2 mm	-13°	-39°	14°	0°
PCH2211	MS687	6 mm	-4°	-24°	6°	1°
PCH2212	MS688	-3 mm	-4°	-21°	14°	8°
PCH2213	MS689	7 mm	-1°	-23°	19°	1°

*2 mm (-3 mm) means the anatomic reference z position is 2mm higher (lower) than the bumper centre z position.

A system of belts equipped with a pretension device was triggered to catch up the subject in order to avoid a second impact on the mini-sled or the ground (more details can be found in Appendix B). In all tests the belts became tensed only after 120 ms. Beyond this time, the pedestrian experienced a free falling because the bonnet and the windshield were not represented in this buck. There was no interest to record the kinematics of this free falling.

Data scaling

All four PMHS tested were different sizes from M50, therefore it was necessary to scale measurements obtained from these subjects in order to establish biofidelity targets for M50. To do this, the following method was applied:

- individual scale factor for each upper body segment trajectory and for each PMHS was applied according to SAE J2868 OCT2010 (Eq. 1–3);
- for trajectories of lower extremities, no scaling was applied since they mainly experienced translational displacement;
- regarding impact forces from the spoiler, bumper and BLE, they were scaled based on leg mass of each PMHS (Eq. 5–10)

$$\lambda_L = \frac{L_{50}}{L} \tag{5}$$

$$displ_{scaled} = displ_{unscaled} \times \lambda_L \tag{6}$$

$$time_{scaled} = time_{unscaled} \times \lambda_L \tag{7}$$

$$\lambda_m = \frac{m_{50}}{m} \tag{8}$$

$$force_{scaled} = force_{unscaled} \times \lambda_m^{2/3} \tag{9}$$

$$time_{scaled} = time_{unscaled} \times \lambda_L \tag{10}$$

where L_{50} and m_{50} are the reference M50 height and leg mass; L and m are corresponding height and leg mass for the subject; λ_L and λ_m are corresponding length and mass scaling factors. Table III gives the length and mass factors calculated for scaling PMHS data to the 50th percentile male pedestrian. Note that the mass scale factors are large due to the fact that the subjects tested were elderly with thin legs.

TABLE IV

LENGTH AND MASS SCALE FACTORS

Test #	Subject #	Height from the ground (mm)									
		HeadL	T1	AcromionL	T4	T12	Sacrum Sup	Sacrum Low	KneeR	AnkleR	Mass (kg)
	Reference*	1676	1516	1511	1459	1230	1085	1025	505	137	13,2
PCH2210	MS686	1618	1538	1470	1484	1213	1065	981	514	171	8,5
PCH2211	MS687	1553	1521	1467	1408	1167	991	924	542	86	10,7
PCH2212	MS688	1671	1585	1568	1528	1265	1086	1027	542	159	10,5
PCH2213	MS689	1571	1507	1477	1432	1163	969	885	498	83	10,1
Test #	Subject #	Length scale									Mass scale factor
PCH2210	MS686	1,036	0,986	1,028	0,983	1,014	1,019	1,045	1,000	1,000	1,5529
PCH2211	MS687	1,079	0,997	1,030	1,036	1,055	1,095	1,109	1,000	1,000	1,2336
PCH2212	MS688	1,003	0,957	0,964	0,955	0,973	0,999	0,998	1,000	1,000	1,2571
PCH2213	MS689	1,067	1,006	1,023	1,019	1,058	1,119	1,158	1,000	1,000	1,3069

*Reference from GHBMC 50th Percentile Male Pedestrian Model in a mid-gait stance wearing shoes of 28 mm.

III. RESULTS

Injury Results

Table V and Table VI report the detailed injuries observed via autopsy. The 2005 AIS severity is also provided.

TABLE V
RIGHT LIMB INJURIES CODED IN AIS 2005. CAPSULE TEAR AND TIBIA PLATEAU FRACTURE ARE INDICATED BY THE SYMBOL "X" BUT NOT CODED.

Right limb						
Test #	Subject #	Highest AIS	MCL rupture*	Tibia fracture	Fibula fracture	Capsule tear
PCH2210	MS686	2	2	0	0	0
PCH2211	MS687	2	2	0	0	0
PCH2212	MS688	2	2	0	0	x
PCH2213	MS689	2	2	2	2	x

*MCL: the medial collateral ligament of the knee.

TABLE VI
LEFT LIMB INJURIES CODED IN AIS 2005. CAPSULE TEAR, TIBIA PLATEAU FRACTURE AND PATELLAR RETINACULUM TEAR ARE INDICATED BY THE SYMBOL "X" BUT NOT CODED.

Left limb							
Test #	Subject #	Highest AIS	LCL rupture*	ACL rupture*	Fibula fracture	Meniscus tear	Capsule tear
PCH2210	MS686	2	2	2	0	2	x
PCH2211	MS687	2	2	0	0	2	0
PCH2212	MS688	2	2	2	0	2	0
PCH2213	MS689	2	2	2	2	2	0

*LCL: the lateral collateral ligament of the knee; ACL: the anterior cruciate ligament of the knee.

Impact forces

Time history plots of the scaled impact forces from the spoiler, bumper and BLE on PMHS are included in Fig. 8.

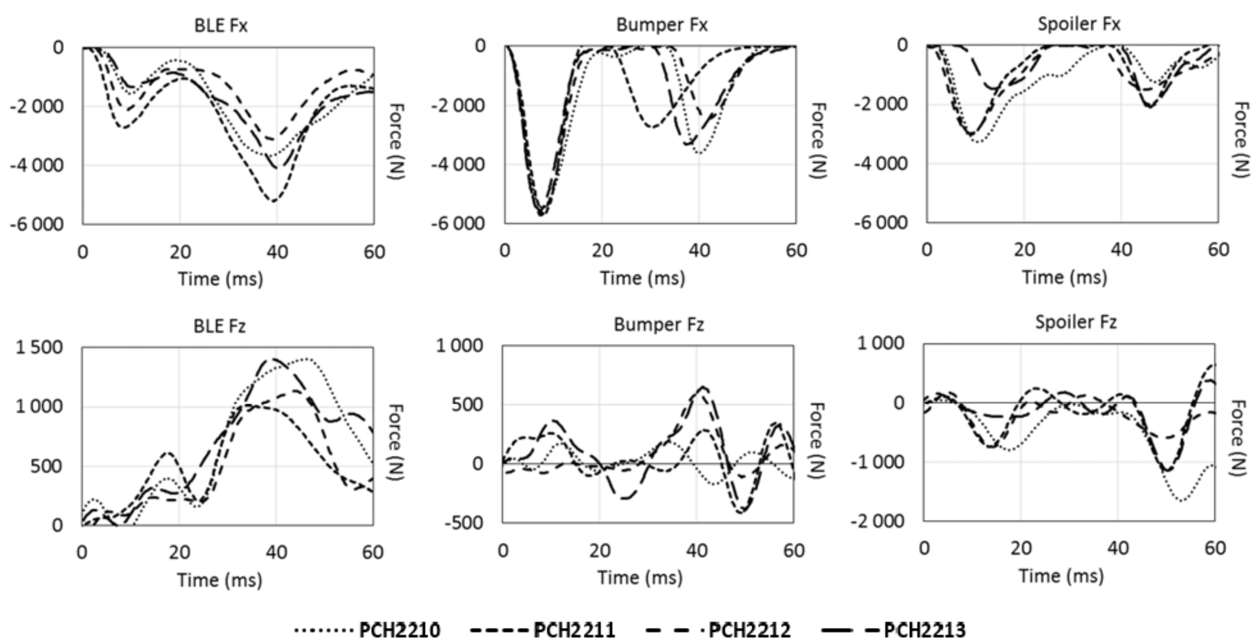

Fig. 8. Time history plots of the scaled impact forces from the spoiler, bumper and BLE on PMHS, expressed in the axes of the laboratory coordinate system. The starting time of the second wave in Bumper Fx and in Spoiler Fx corresponds to the contact time of the contralateral limb with the buck.

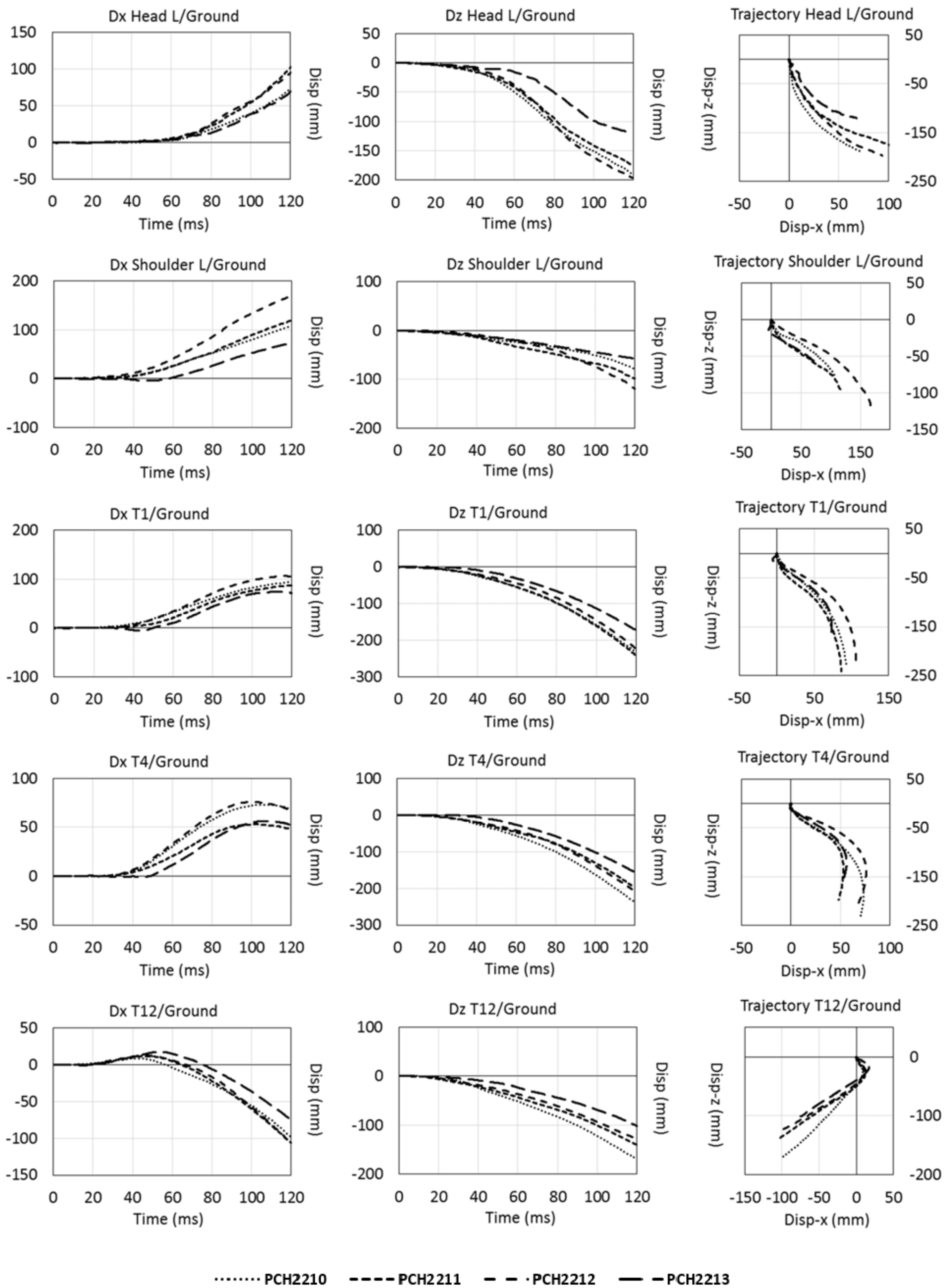

Fig. 9. Time history plots of the scaled displacement of the head, shoulder, T1, T4, T12, as well as corresponding trajectories with respect to the ground, expressed in the axes of the laboratory coordinate system.

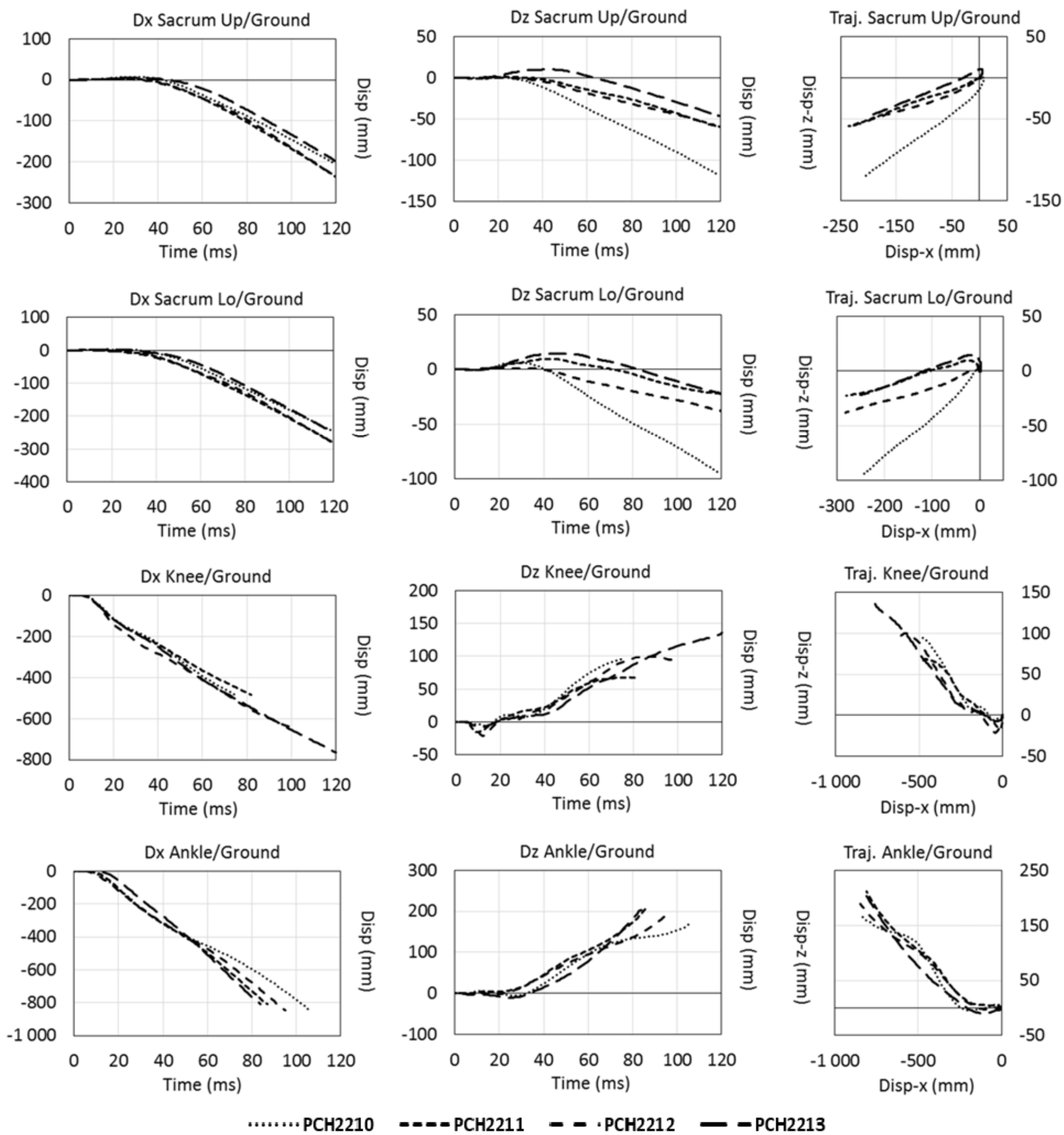

Fig. 10. Time history plots of the scaled displacement of the upper sacrum, lower sacrum, knee, ankle, as well as corresponding trajectories with respect to the ground, expressed in the axes of the laboratory coordinate system.

IV. DISCUSSION

A generic vehicle buck was used to perform pedestrian tests in this study. It was developed based on a mid-size European sedan. Figure 11 shows its geometry compared to the front end of the sedan. The stiffness of the tubes was defined in order to be as close as possible to the stiffness of the same sedan. Besides, the relative position between the tubes changed proportionally in function of the thigh and lower leg lengths, which allowed impacting the pedestrian legs in a similar way. The authors did not seek to develop a generic vehicle buck with mean shape and stiffness of actual vehicles. In fact, to validate a dummy or a computational human body model, one need various tests conditions, using different loading shape and stiffness, different impact velocity and angles. A validation study would be quite limited if it was performed only with a mean vehicle shape and stiffness and a unique impact velocity of 11.1 m/s. This study went along with this consideration by providing PMHS responses against a particular vehicle shape and stiffness and with an impact velocity of 8 m/s. This consideration is also valid regarding injury risk curve construction which needs different levels of impact severity, while almost all pedestrian tests in literature were realized with an impact velocity of 11.1 m/s

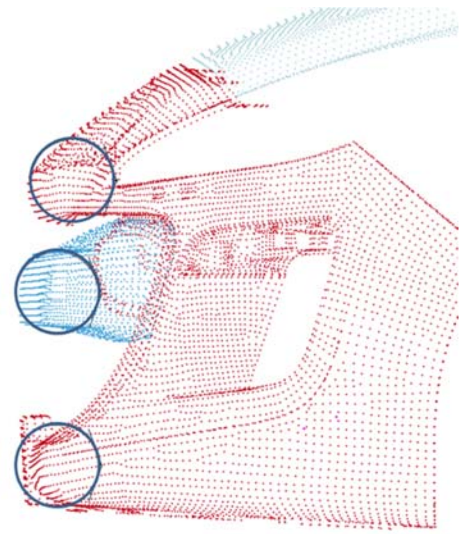

Fig. 11. Comparison of the buck shape (represented by the three cylindrical tubes) with respect to a mid-size European sedan.

In this study, the GHBMC 50th percentile simplified pedestrian model (GHBMC_M50_PS) [11] was used as a representation of the 50th percentile male pedestrian (M50) in order to position PMHS, to scale kinematic responses and to illustrate the test set-up and instrumentations used. This choice was made based on three considerations. First, the model geometry corresponds to a selected volunteer who closely matched the average-sized male individual from two anthropomorphic studies [12-13], showing an average 3% difference between all external anthropometry values for the 50th percentile male identified in Gordon *et al.* [14], according to Gayzik *et al.* [13]. Secondly, it is easier to get all anatomic dimensions using the model and to position the subjects and to scale their responses to the 50th percentile male. Thirdly, it allows direct evaluation of the GHBMC_M50_PS model with respect to the scaled responses.

To position the human subjects, our method was firstly to define the theoretical relative position of a M50 with respect to the buck (showed in Fig.6). To define this theoretical relative position, the best way was to use the GHBMC M50-PS model, to position it in frontal of the buck model and to determine their relative position. Thus, it was determined that the bumper tube centre was located 10 mm under the right knee reference point (which is the tibia plateau and centered relative to the anterior and posterior edges of the tibia plateau). This right knee target was referred to as the anatomical reference in this study. Then, for all actual subjects who were not M50, they remained impacted by the bumper with its centre 10 mm under the anatomic reference, but the relative position of the BLE and the spoiler with respect to the bumper was scaled proportionally according to Equations (1)-(6). In this way, the impact positions on the legs were proportionally comparable between different subjects, and consequently the pedestrian responses were more consistent to construct corridors.

The injury for the right limb (first impacted) is essentially relative to the MCL rupture (4/4). Only one specimen (MS689) sustained tibia and fibula fractures. Regarding the left limb, the LCL ruptured systematically (4/4), followed by the ACL (3/4). Furthermore, meniscus tear was also present for all four specimens, and fibula fracture was only observed for one specimen (MS689). This high frequency of knee injury and relatively low frequency of leg fractures was also observed by Kerrigan *et al.* In their study they compared laboratory pedestrian experiments versus field data, and found that PMHS, contrary to field data, sustained a high frequency of knee injury and relatively low frequency of leg fractures. They advanced two possible explanations for this discrepancy. First, the higher muscular strength of field pedestrian may provide increased bending stiffness of the knee joint, resulting in leg fracture prior to knee joint injury. Secondly, the PMHS were positioned to cause perfectly lateral loading from the vehicle whereas such conditions are probably rare in the field data.

The impact force at the bumper level exhibited no dispersion through the four tests for the first wave, but more dispersion appeared for the second wave in terms of timing. The shape of the BLE impact force was very similar across the four tests, but there was more peak force dispersion. Regarding the impact at the spoiler level, the test with MS689 was very different from the others: the impact force got started 7 ms later and rose up to only 1500 N, compared to 3000 N for the others. To explain this difference, Fig. 12 shows the relative position between the subjects and the tubes. One can observe that the right lower leg of MS689 inclined inwards compared to the others, which inclined outwards. This difference may be the cause of this later response observed in the test with MS689. More generally, it is interesting to study how the leg position and orientation influence the contact forces and trajectories. This can will be investigated in the future by means of personalized human body simulations. Such simulations would also allow to evaluate the scaling procedure used in this study.

It is also to be noted that: (1) the vertical impact force component was very small at the bumper level; (2) the spoiler always exercised a downward pushing force on the lower leg; and (3) the BLE always pushed the pedestrian upwards. The legs inclined due to the impact by the buck, and this inclination led to the vertical force components.

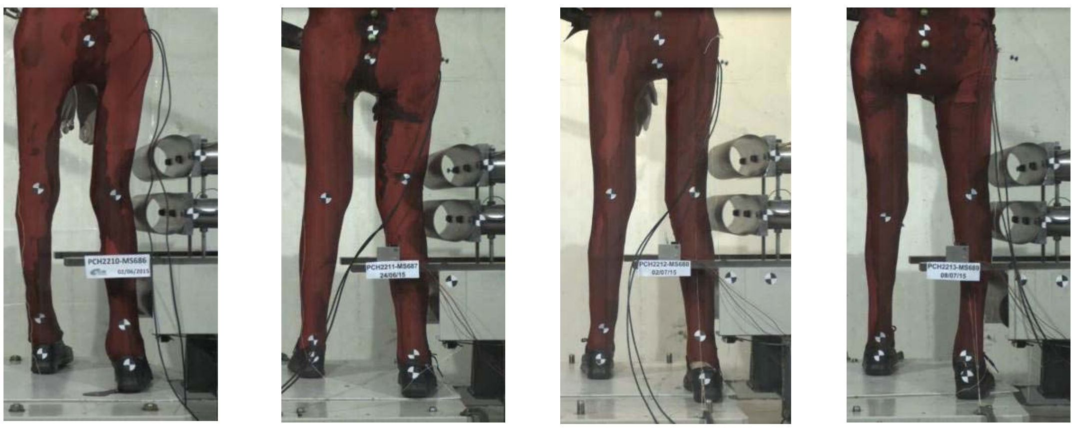

MS 689 MS 687 MS 688 MS 689

Fig. 12. Leg volume and shape difference between the four specimens.

We chose to present kinematics of pedestrian with respect to the ground because this allows better characterization of the horizontal motion of the upper body targets. In fact, these motions would be largely dissimulated by the dominance of the vehicle motion if they were expressed with respect to the vehicle. However, these kinematics were also expressed with respect to the buck and are included in the Appendix (Fig. A1) to highlight the horizontal motion of the lower body targets for similar reasons.

These tests have the advantage that they can be easily duplicated due to the simplicity of the buck developed, and therefore can be used to evaluate biofidelity of pedestrian dummies or computational models. However, their uses are limited to studying pedestrian kinematics and its leg interaction with the buck, as no bonnet and windshield were physically represented to generate data relative to the impact on the pelvis, the thorax and the head. It is to be noted that all time histories measured in these tests were presented in the time window [0-120] ms within which the data can be used despite of the bonnet and windshield. Beyond this window, the responses of the subjects may be affected by the catching system, and its kinematics was similar to free falling and did not represent any interest for biofidelity validation.

Another limitation of the buck is that its mass (150 kg) was much lighter than actual cars and was decelerated after a free race of 650 mm. Simulations with the GHBMC 50th percentile simplified pedestrian model were performed using both the current buck and the same buck but without a constant velocity of 8 m/s. Figure 13 shows the deformation energy time history during the impact. At the end of impact (around 60 ms), the deformation energy was 642 J with the current buck compared to 750 J with the same buck and constant velocity. The deformation energy was only 14% lower with the current test condition. This means that the test conditions used in this study are not so deviated from those with actual cars

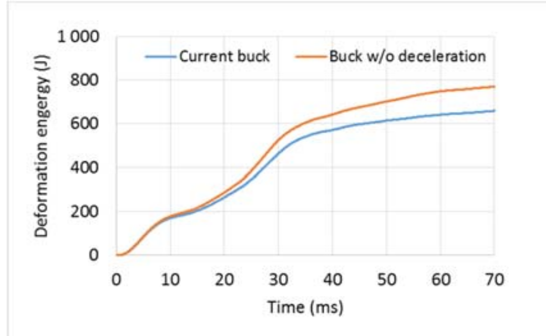

Fig. 13. The deformation energy time history with the current test conditions compared to that with the same buck but with a constant velocity of 8 m/s; results based on simulations with the GHBMC 50th percentile simplified pedestrian model.

Although strain gauges were installed on the right leg bones, the strain measurements were not provided in this paper. Additional work, such as bending tests in order to relate strain measurements to moments in femur sections, is needed to make these measurements usable. These data will be published when they become available.

V. CONCLUSIONS

Four PMHS tests were performed using a simplified vehicle buck at 8 m/s. Whole kinematics and impact forces were recorded, and then scaled to establish a set of biofidelity targets for the 50th percentile male pedestrian. Detailed injury outcomes of PMHS tested were also provided. The simplicity of the buck makes duplication of these tests much easier both for physical tests and for numerical simulations.

VI. ACKNOWLEDGEMENT

The authors would like to acknowledge the donors, whose generosity allowed this study to be carried out.

VII. REFERENCES

[1] Kajzer, J., Schroeder, G., Ishikawa, H., Matsui, Y., Bosch, U. (1997) Shearing and bending effects at the knee joint at high speed lateral loading. *Stapp Car Crash Conference,* **41**: pp.151–65.

[2] Bose, D., *et al*. (2004) Response of the knee joint to the pedestrian impact loading environment. *SAE 2004 World Congress,* SAE Technical Paper #2004-01-1608.

[3] Kerrigan, J. R., *et al*. (2005) Kinematic Corridors for PMHS Tested in Full-Scale Pedestrian Impact Tests. *Proceedings of the 19th International Technical Conference on the Enhanced Safety of Vehicles (ESV),* 2005, Paper 05-0394.

[4] Kerrigan,, J. R., Crandall, J. R., Deng, B. A. (2008) Comparative Analysis of the Pedestrian Injury Risk Predicted by Mechanical Impactors and Post Mortem Human Surrogates. *Stapp Car Crash Journal,* **52**: pp.527–67.

[5] Kerrigan, J. R., Rudd, R. W., Subit, D., Untaroiu, C. D., Crandall, J. R. (2008) Pedestrian Lower Extremity Response and Injury: Small Sedan vs. Large SUV. *SAE Transactions: Journal of Passenger Cars,* **1**(1): pp.985–1002. Based on SAE World Congress Paper 2008-01-1245.

[6] Pipkorn, B., *et al*. (2012) Development and validation of a generic universal vehicle front buck and a demonstration of its use to evaluate a hood leading edge bag for pedestrian protection. *Proceedings of the IRCOBI Conference,* 2012, pp.168–81.

[7] Pipkorn, B., *et al*. (2014) Development and component validation of a generic vehicle front buck for pedestrian impact evaluation. *Proceedings of the IRCOBI Conference,* 2014, pp.718–29.
[8] Takahashi, Y., *et al*. (2014) Fullscale validation of a generic buck for pedestrian impact simulation. *Proceedings of the IRCOBI Conference,* 2014, pp.730–45.
[9] Forman, J. L., *et al*. (2015) Biofidelity corridors for whole-body pedestrian impact with a generic buck. *Proceedings of the IRCOBI Conference,* 2015.
[10] Forman, J. L., *et al.* (2015) Whole-body Response for Pedestrian Impact with a Generic Sedan Buck. *Stapp Car Crash Journal,* **59**: pp.401–44.
[11] Untaroiu, C. D., Putnam, J. B., Schap, J., Davis, M. L., Gayzik, F. (2015) Development and Preliminary Validation of a 50th Percentile Pedestrian Finite Element Model. ASME. International Design Engineering Technical Conferences and Computers and Information in Engineering Conference, Volume 3: 17th International Conference on Advanced Vehicle Technologies; 12th International Conference on Design Education; 8th Frontiers in Biomedical Devices:V003T01A004. doi:10.1115/DETC2015-47781.
[12] Schneider, L., Robbins, D., Pflug, M. and Snyder, R. (1983) Development of Anthropometrically Based Design Specifications for an Advanced Adult Anthropometric Dummy Family. United States Department of Transportation, National Highway Traffic Safety Administration, DOT/HS806 715, Vol. 1.
[13] Gordon, C. C., *et al*. (1988) Anthropometric Survey of U.S. Army Personnel: Methods and Summary Statistics. 1989 Technical Report: Natick/TR-89/044. Prepared for United States Army Natick Research, Development and Engineering Center, Natick, MA.
[14] Gayzik, F. S., *et al*. (2012) External landmark, body surface, and volume data of a mid-sized male in seated and standing postures. *Annals of Biomedical Engineering*, **40**(9): pp.2019–32.

VIII. APPENDIX

Appendix A:

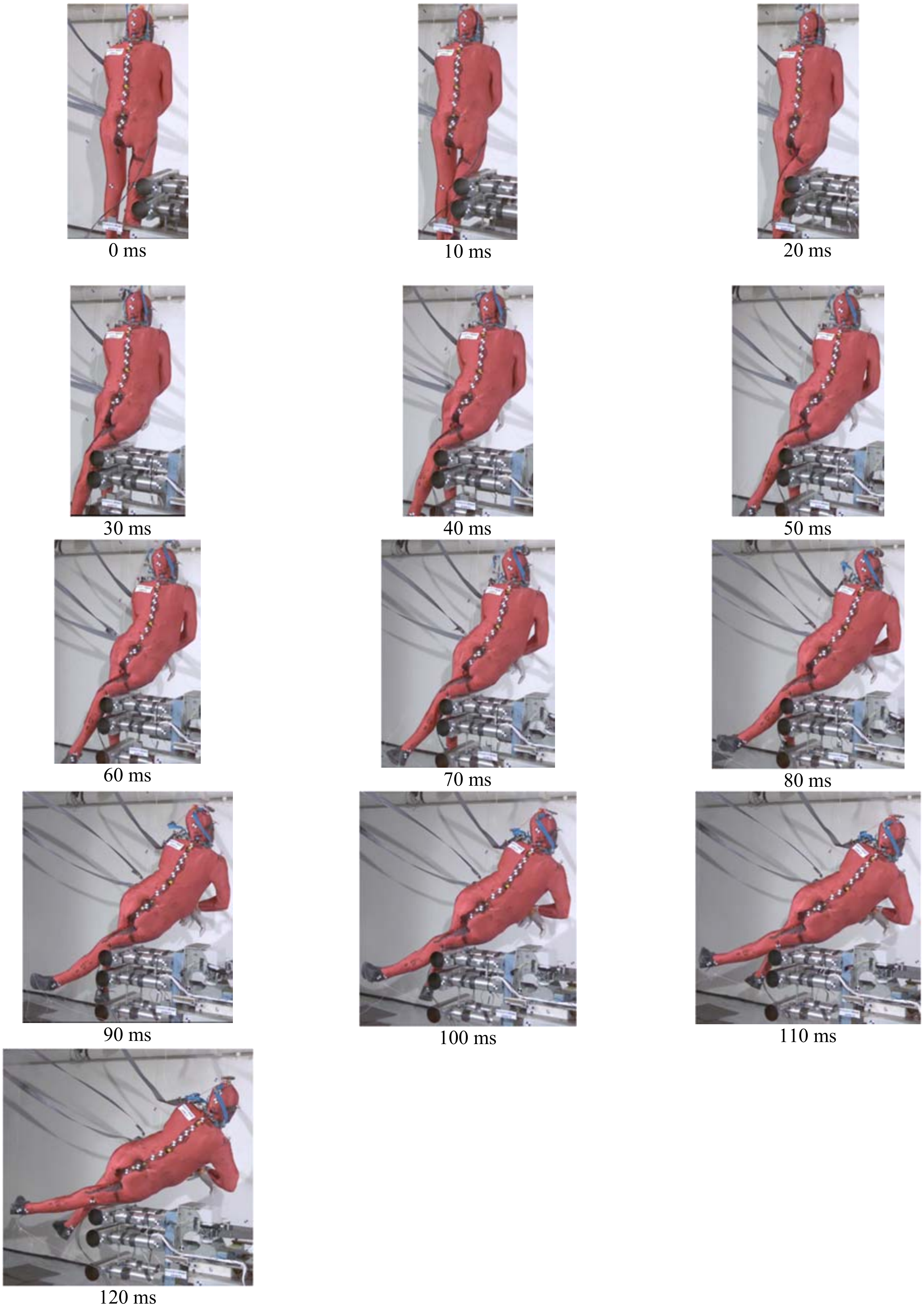

Fig. A1. Still captures from the high-speed video for Test PCH2211-MS687.

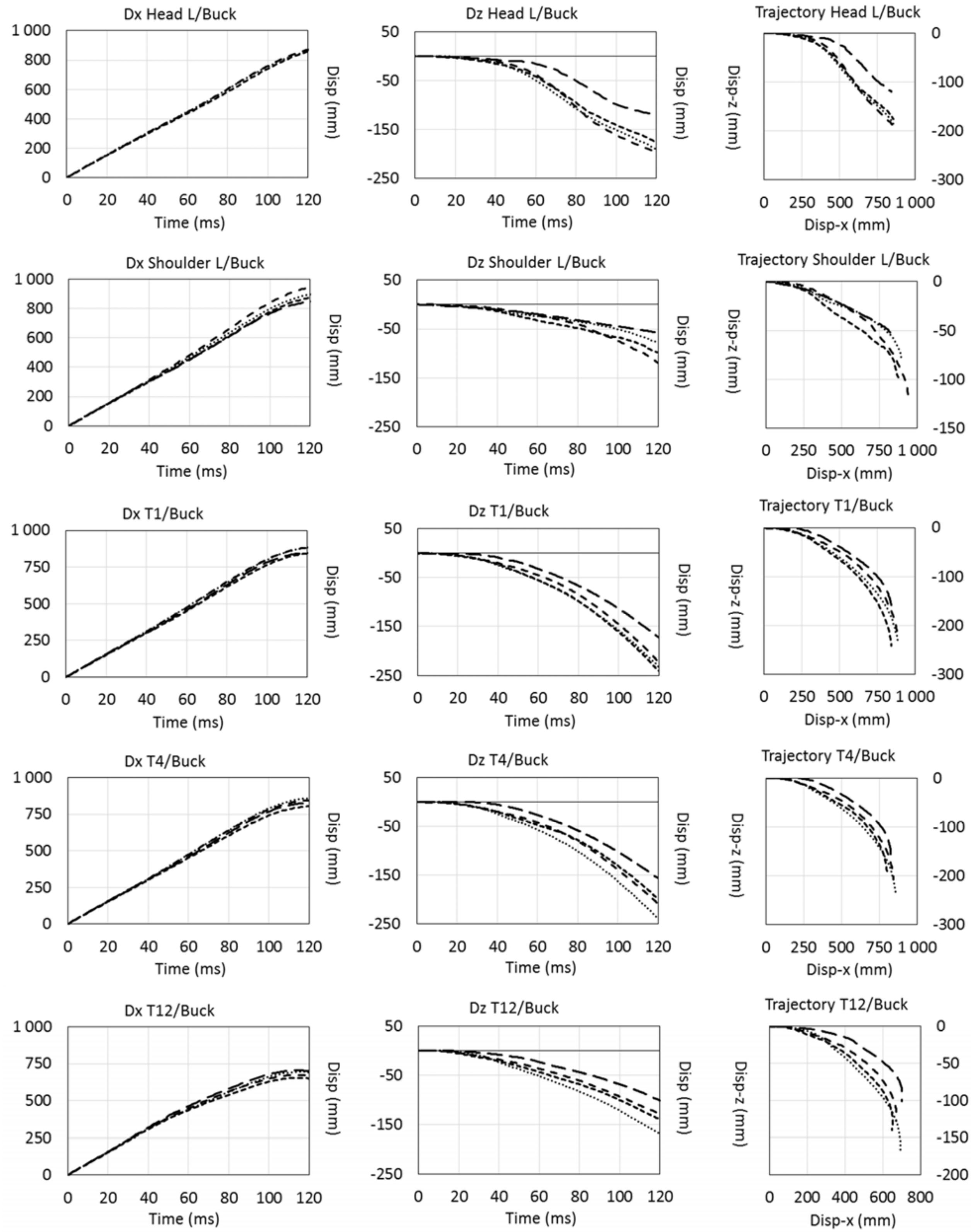

Fig. A2. Time history plots of the scaled displacement of the head, shoulder, T1, T4, T12, as well as corresponding trajectories with respect to the buck, expressed in the axes of the laboratory coordinate system.

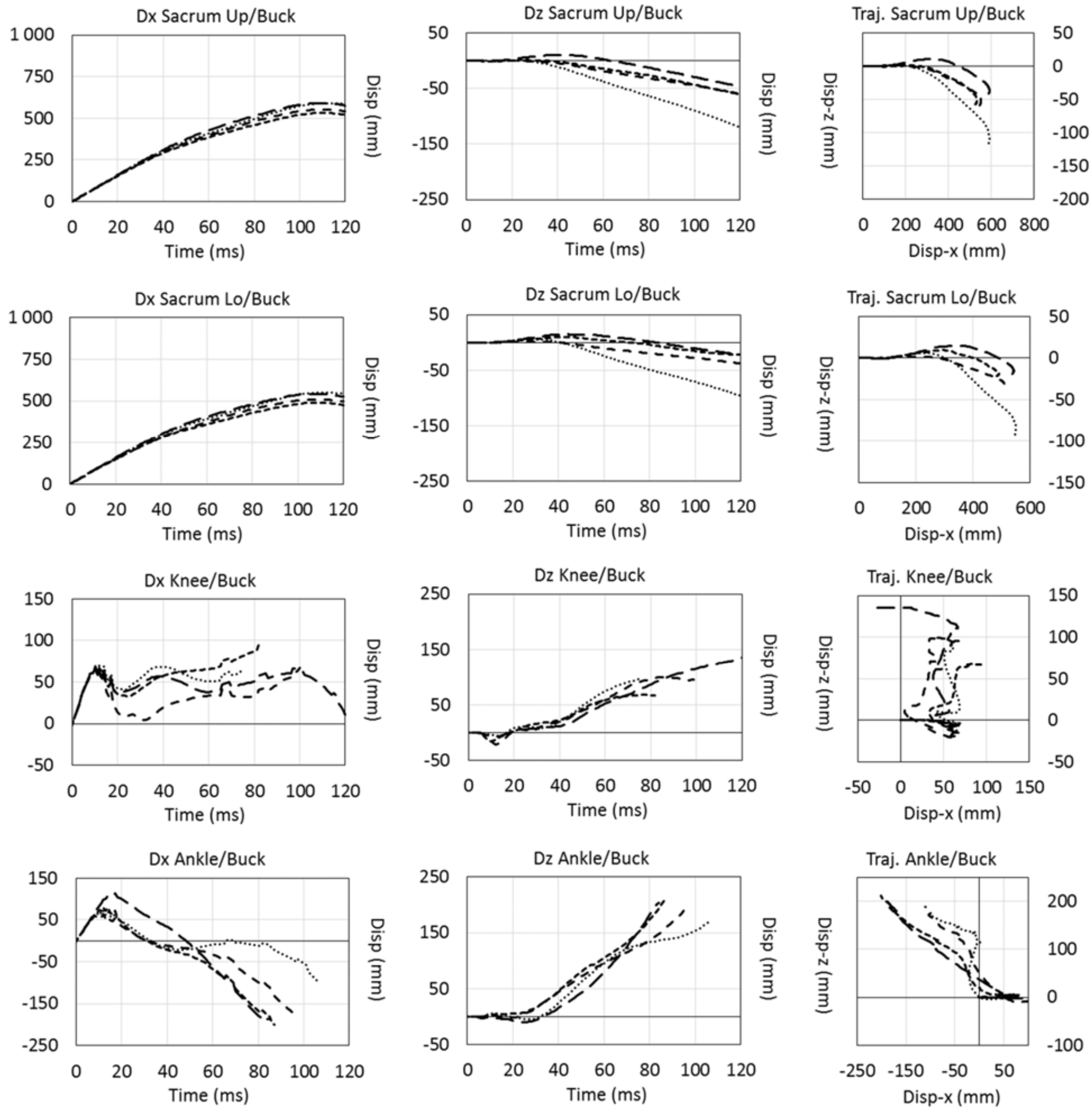

Fig. A3. Time history plots of the scaled displacement of the upper sacrum, lower sacrum, knee, ankle, as well as corresponding trajectories with respect to the buck, expressed in the axes of the laboratory coordinate system.

Appendix B: Pedestrian catching system

At the end of loading on the pedestrian (120 ms after the beginning of the impact), its motion was controlled by a catching system (Figure B1) in order to avoid a second impact between the subject, the mini-sled and the ground. The system was composed of two parts.

- Shoulder belt: A belt equipped with a load limiter of 600 kN and a pyrotechnic pretensioner was attached to the shoulder. Its length was 1100 mm minus a half of the shoulder breadth. The pretension was activated when the mini-sled started coming back.

- Pelvis belt: Two belts, each equipped with a load limiter of 400 kN and a pyrotechnic pretensioner, were attached to the pelvis. One pyrotechnic pretensioner was activated when the pelvis was moved 1000 mm forward, and the second at 300 ms after the initial impact.

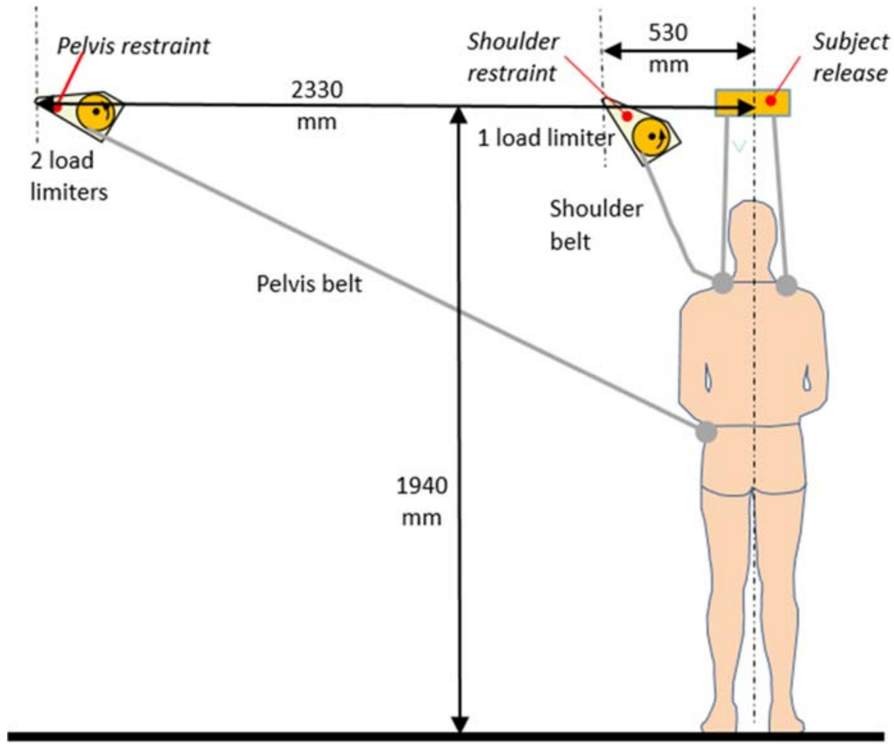

Fig. B1. Pedestrian catching system